 doi:10.20944/preprints201905.0100.v1

Thermodynamic Assessment and Multi-Objective Optimization of Performance of Irreversible Dual-Miller Cycle

Shahryar Abedinnezhad[1], Mohammad Hossein Ahmadi[2], Seyed Mohsen Pourkiaei[3], Fathollah Pourfayaz[3], Amir Mosavi [4,5] , Michel Feidt [6], Shahaboddin Shamshirband[7,8*]

[1] Department of Mechanical Engineering, Sharif University of Technology, Tehran, Iran

[2] Faculty of Mechanical Engineering, Shahrood University of Technology, Shahrood, Iran

[3] Department of Renewable Energy and Environmental Engineering, University of Tehran, Tehran, Iran

[4] School of the Built Environment, Oxford Brookes University, Oxford OX3 0BP, UK,

[5] Faculty of Health, Queensland University of Technology, Brisbane QLD 4059, Australia

[6] University of Lorraine, LEMTA, 2 avenue de la forêt de Haye 54516 Vandoeuvre les Nancy, France

[7] Department for Management of Science and Technology Development, Ton Duc Thang University, Ho Chi Minh City, Vietnam

Corresponding author Email: shahaboddin.shamshirband@tdt.edu.vn (S.Shamshirband)

Abstract

Although different assessments and evaluations of Dual-Miller cycle performed, specified output power and thermal performance associated with engine determined. Besides, multi objective optimization of thermal efficiency, Ecological Coefficient of performance ($ECOP$) and Ecological function (E_{un}) by the mean of NSGA-II technique and thermodynamic analysis performed. The Pareto optimal frontier obtaining the best optimum solution is chosen by fuzzy Bellman-Zadeh, LINMAP, and TOPSIS decision-making techniques.

Based on the results, performances of dual-Miller cycles and their optimization are improved.

Keywords: Dual-Miller cycle; thermodynamic analysis; power; ecological coefficient of performance; thermal efficiency; entropy generation; multi-objective optimization

Nomenclature

DMC	Dual-Miller cycle
m	Mass flow rate
n	Polytropic exponent
k	The specific heat ratio (adiabatic exponent)
P	Power
Q	Heat
T	Temperature
$ECOP$	Ecological Coefficient of Performance
E_{un}	Ecological function
V	volume
C_v	The specific heat at constant volume
C_p	The specific heat at constant pressure
σ_{un}	total entropy generation
η	Efficiency
r_M	The Miller cycle ratio of a Dual-Miller cycle
ρ	The cut-off ratio
λ	The pressure ratio
ε	The compression ratio

1. Introduction

FTT is one of the most reliable optimization tools to assess the performance of internal combustion engine cycles (ICEC) [1–13]. Recent studies of thermodynamic systems [14–23], comprehensive investigations have been carried out [24]. Entropy optimization [25–29], E_{un} criterion [30–34] and $ECOP$ criterion [35–40] are some of the recent various optimization objectives in ICEC analysis. Generally, entropy reduction is not equal to enhancing thermal efficiency or maximum power generation. Under certain circumstances, minimizing entropy generation leads to the highest power generation [41]. Blank et al. [42] investigated the efficiency of an endoreversible air standard dual cycle considering the system heat loss. Chen and colleagues [43] investigated an air standard dual cycle taking the friction and heat loss into account. Ust and colleagues [44] conducted a performance optimization for an irreversible air standard dual cycle taking the impact of heat loss and internal irreversibility into account. Ghatak et al. [45] analyzed the performance of an endoreversible air standard dual cycle considering thermal characteristics of the working fluid. Wang et al. [46] carried out a performance analysis considering the finite-time element and internal loss. Ge and colleagues [47] performed a thermodynamic analysis of an irreversible air standard dual cycle. In the thermodynamic assessment and optimization of air standard Miller cycles, Al-Sarkhi and colleagues [48] optimized the power density of a reversible cycle. Chen and colleagues [49,50] assessed the efficiency of an irreversible air standard Miller cycle considering thermal properties of the working fluid and friction and heat loss of the system. Lin and colleagues [51] conducted an optimization for an irreversible air standard Miller system. Due to the thermodynamic evaluation of single cycles, Gonca et al. and other researchers [52-58] and Gonca [59] analyzed irreversible Dual-Miller cycles taking the power and thermal efficiency into account. Ust and colleagues [60] conducted an exergy optimization for an irreversible Dual-Miller cycle. Gonca and colleagues [61,62] analyzed the $ECOP$ of an irreversible Dual-Miller cycle. Wu and colleagues [63,64] investigated the efficiency of an irreversible Dual-Miller cycle considering linear [63] and nonlinear [64] thermal properties of working fluid. Huleihil et al. [65] presented and evaluated a reversible air standard Otto model through polytropic processes. Gong and colleagues [66] performed a performance optimization of an endoreversible Lenoir cycle considering heat losses and polytropic processes. Also, Xiong and colleagues [67] conducted a performance optimization of an endoreversible air standard Otto cycle considering heat losses and polytropic processes. Zhang and colleagues [68] designed and evaluated an irreversible universal cycle model, considering heat and friction losses, polytropic stages, and thermal properties of the working fluid.

 doi:10.20944/preprints201905.0100.v1

Multi-objective optimization is a valuable method to overcome various engineering difficulties [69-71]. Answering a multi-objective optimization question needs simultaneous substantiation of various objectives. Consequently, evolutionary algorithms presented and advanced to answer multi-objective problems applying various methods [72]. A proper approach to find a solution to for a multi-objective problem is to examine a group of routes, each satisfies the objectives at an acceptable level and do not interfere with other routes [73]. Multi-objective optimization problems generally represent a practicably numerous collection of routes named frontier of Pareto, which examined vectors show the possible primary connections in the whole area of the objective function. New studies indicate that multi-objective optimizations for different thermodynamic cycles applied in various engineering problems [74-101].

In this study, investigated the performance of Irreversible Dual-Miller Cycle. Also, the presented effect of critical parameters on the performance of Dual-miller cycle. Key parameters that presented include ε, ρ and the n. The effects of these parameters on the power, efficiency, $ECOP$ and E_{un} of the system evaluated. Then done multi-objective optimization to obtain the best point of performance of Dual-Miller Cycle.

2. Dual-Miller cycle through a polytropic stage

An air standard Dual-Miller cycle is presented in Fig.1. To increase the accuracy of performance assessment, the polytropic process replaces by the reversible adiabatic stage, which is impractical to attain in the improved Dual-Miller cycle [64]. As it is depicted in Figure 1, cycle 1–2–3–4–5–6–1 represents the condition in which n=k.

Preprints (www.preprints.org) | NOT PEER-REVIEWED | Posted: 9 May 2019 doi:10.20944/preprints201905.0100.v1

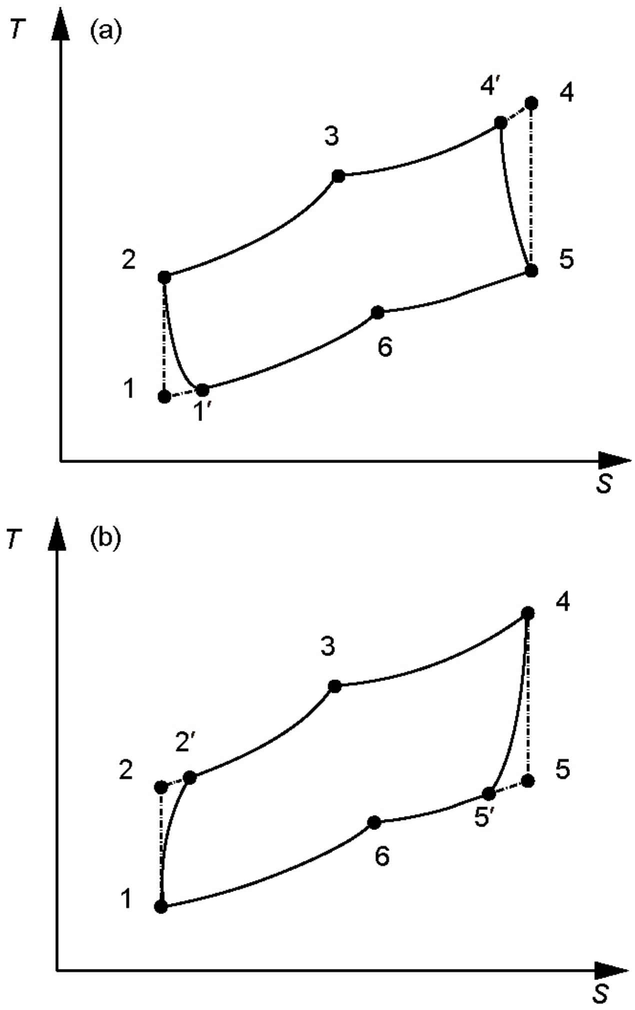

Fig.1 *T-S* diagram of DMC: *n* less than *k* (a) and *n* higher than *k* (b) [102].

2.1 Ideal air standard Dual-Miller cycle

In ideal gas systems (*n* equal to *k*), the state elements of each stage can be practically obtained, by the ideal gas state equation. The first law of thermodynamics clear that the heat transfer rates and power generation of the cycle can be determined. Equation (1) presents ε, λ, ρ and r_M, respectively:

$$\varepsilon = \frac{V_1}{V_2}, \lambda = \frac{P_3}{P_2}, \rho = \frac{V_4}{V_3}, r_M = \frac{V_6}{V_1} \tag{1}$$

The primary thermodynamic equations of each stage defined as:

$$T_2 = T_1 \varepsilon^{k-1} \tag{2}$$

$$T_3 = T_2 \lambda \tag{3}$$

Preprints (www.preprints.org) | NOT PEER-REVIEWED | Posted: 9 May 2019 doi:10.20944/preprints201905.0100.v1

$$T_4 = T_3 \rho \quad (4)$$

$$T_5 = T_4 \left(\frac{\rho}{\varepsilon . r_M} \right)^{k-1} \quad (5)$$

$$T_6 = T_5 \left(\frac{r_M^k}{\lambda . \rho^k} \right) \quad (6)$$

$$T_1 = \frac{T_6}{r_M} \quad (7)$$

The heat transfer ratios of the system fluid are as follows:

$$Q_{in} = Q_{23} + Q_{34} = \dot{m}(C_v (T_3 - T_2) + C_p (T_4 - T_3)) \quad (8)$$

$$Q_{out} = Q_{56} + Q_{61} = \dot{m}(C_v (T_5 - T_6) + C_p (T_6 - T_1)) \quad (9)$$

In the ideal reversible air standard Dual-Miller cycle, the heat transfer impact is not considered, while it considered for an actual DMC. This waste is considered relevant to the temperature difference of working fluid and the cylinder wall as follows [102,103]

$$Q_l = \frac{B}{2}(T_2 + T_4 - 2T_0) \quad (10)$$

The power production and performance are calculated as:

$$P = Q_{in} - Q_{out} \quad (11)$$

$$\eta = \frac{P}{Q_{in} + Q_l} \quad (12)$$

2.2 Air standard Dual-Miller cycle

As it is depicted in Fig.1, T1 in a Dual-Miller cycle (*n* less than k*)*, is higher than the T1 in air standard Dual-Miller cycle. In order to keep T2 fixed through the compression stage, heat must be extracted through the polytropic stage 1'–2. Considering heat waste through the heat input stage, T4' is lower than T4. In order to keep T5 fixed, heat should be increased through the polytropic stage 4'–5.

The equations of each stage are defined as:

$$T_2 = T_{1'} \varepsilon^{\left(\frac{k(n-1)}{n} \right)} \quad (13)$$

Preprints (www.preprints.org) | NOT PEER-REVIEWED | Posted: 9 May 2019 doi:10.20944/preprints201905.0100.v1

$$T_5 = T_{4'} \left(\frac{\rho}{\varepsilon . r_M} \right)^{\frac{k(n-1)}{n}} \tag{14}$$

The heat transfer rate of polytropic stage 1'–2, is defined as follows:

$$Q_{1'2} = \dot{m} C_v \left(\frac{k-n}{n-1} \right) (T_2 - T_{1'}) \tag{15}$$

The heat transfer rate of stages 2–3 and 3–4', are defined as follows:

$$Q_{23} = \dot{m} C_v (T_3 - T_2) \tag{16}$$

$$Q_{34'} = \dot{m} C_p (T_{4'} - T_3) \tag{17}$$

The heat transfer rate of stage 4'–5, is defined as follows:

$$Q_{4'5} = \dot{m} C_v \left(\frac{k-n}{n-1} \right) (T_{4'} - T_5) \tag{18}$$

The heat transfer rate of stages 5–6 and 6–1', are defined as follows:

$$Q_{56} = \dot{m} C_v (T_5 - T_6) \tag{19}$$

$$Q_{61'} = \dot{m} C_p (T_6 - T_{1'}) \tag{20}$$

The heat input of the cycle is

$$Q_{in1} = Q_{23} + Q_{34'} + Q_{4'5} \tag{21}$$

The heat output of the cycle is

$$Q_{out1} = Q_{1'2} + Q_{56} + Q_{61'} \tag{22}$$

For an ideal air standard Dual-Miller cycle, the ratio of the highest temperature to the lowest temperature is defined as follows:

$$\frac{T_4}{T_1} = \rho . \lambda . \varepsilon^{k-1} \tag{23}$$

As stated by the ref. [102,103], the heat waste ratio is defined as follows:

$$Q_{l1} = \frac{B}{2} (T_2 + T_{4'} - 2T_0) \tag{24}$$

Preprints (www.preprints.org) | NOT PEER-REVIEWED | Posted: 9 May 2019 doi:10.20944/preprints201905.0100.v1

As a result, the generated power and the first law efficiency of the system are defined as follows:

$$P_1 = Q_{in1} - Q_{out1} \tag{25}$$

$$\eta_1 = \frac{P_1}{Q_{in}} = \frac{P_1}{Q_{23} + Q_{34'} + Q_{4'5} + Q_{l1}} \tag{26}$$

Considering the assumption in ref. [104], the exhaust gas recirculation due to the heat transfer loss is determined as follows:

$$\sigma_{q1} = \frac{B(T_2 + T_{4'} - 2T_0)}{2T_0} \tag{27}$$

The exhaust gas recirculation due to the working fluid heat rejection is defined as [105]:

$$\sigma_{pq1} = m\left(\int_{T_{1'}}^{T_6} C_p\left(\frac{1}{T_0} - \frac{1}{T}\right)dT + \int_{T_6}^{T_5} C_v\left(\frac{1}{T_0} - \frac{1}{T}\right)dT + \int_{T_{1'}}^{T_2} C_v\left(\frac{k-n}{n-1}\right)\left(\frac{1}{T_0} - \frac{1}{T}\right)dT\right) \tag{28}$$

As a result, the total entropy generation (σ_{un1}) of the system is defined as follows:

$$\sigma_{un1} = \sigma_{q1} + \sigma_{pq1} \tag{29}$$

According to refs. [30–34], $ECOP$ of the cycle is defined as follows:

$$ECOP = \frac{P_1}{T_0 \sigma_{un1}} \tag{30}$$

According to references. [30–34], E_{un} is defined as follows:

$$E_{un1} = P_1 - T_0 \sigma_{un1} \tag{31}$$

2.3 Air standard Dual-Miller cycle

As it is depicted in Fig.2, T2 the highest temperature of the adiabatic stage 1–2 is less than that of the polytropic stage, due to the heat waste through the isochoric stage 2–3 (*n* higher than *k*). Thus, more heat should be applied through the polytropic stage 1–2'. On the other hand, heat is extracted through the stage 4–5' as T5 the minimum temperature of the adiabatic stage 4–5 is greater than that of the polytropic stage 4–5' taking the heat waste through the isobaric stage 3–4, into account.

The equations of polytropic stages are defined as follows:

$$T_{2'} = T_1 . \varepsilon^{n-1} \tag{32}$$

$$T_{5'} = T_4 . (\frac{\rho}{\varepsilon . r_M})^{n-1} \tag{33}$$

For polytropic stage 1–2', the heat transfer ratio is defined as:

$$Q_{12'} = \dot{m} C_v (\frac{n-k}{n-1})(T_{2'} - T_1) \tag{34}$$

For stages 2'–3 and 3–4, heat transfer rates are defined as:

$$Q_{2'3} = \dot{m} C_v (T_3 - T_{2'}) \tag{35}$$

$$Q_{34} = \dot{m} C_p (T_4 - T_3) \tag{36}$$

For stage 4–5', the heat transfer rate is defined as:

$$Q_{45'} = \dot{m} C_v (\frac{n-k}{n-1})(T_4 - T_{5'}) \tag{37}$$

For stages 5'–6 and 6–1', heat transfer rates are defined as:

$$Q_{5'6} = \dot{m} C_v (T_{5'} - T_6) \tag{38}$$

$$Q_{61} = \dot{m} C_p (T_6 - T_1) \tag{39}$$

The net heat input ratio is calculated as:

$$Q_{in2} = Q_{12'} + Q_{2'3} + Q_{34} \tag{40}$$

The net heat output ratio is calculated as:

$$Q_{out2} = Q_{45'} + Q_{5'6} + Q_{61} \tag{41}$$

The heat waste ratio is calculated as [102,103]:

$$Q_{l2} = \frac{B}{2}(T_{2'} + T_4 - 2T_0) \tag{42}$$

The power generation and the first law efficiency of the system are defined as follows:

$$P_2 = Q_{in2} - Q_{out2} \tag{43}$$

$$\eta_2 = \frac{P_2}{Q_{in}} = \frac{P_2}{Q_{12'} + Q_{2'3} + Q_{34} + Q_{l2}} \tag{44}$$

The exhaust gas recirculation of the heat transfer loss is calculated as follows [104]:

$$\sigma_{q2} = \frac{B(T_{2'} + T_4 - 2T_0)}{2T_0} \tag{45}$$

The exhaust gas recirculation due to the working fluid heat rejection is as follows [105]:

$$\sigma_{pq2} = m\left(\int_{T_{1'}}^{T_6} C_p\left(\frac{1}{T_0} - \frac{1}{T}\right)dT + \int_{T_6}^{T_{5'}} C_v\left(\frac{1}{T_0} - \frac{1}{T}\right)dT + \int_{T_{5'}}^{T_4} C_v\left(\frac{n-k}{n-1}\right)\left(\frac{1}{T_0} - \frac{1}{T}\right)dT\right) \tag{46}$$

The total exhaust gas recirculation of the system is defined as follows:

$$\sigma_{un2} = \sigma_{q2} + \sigma_{pq2} \tag{47}$$

According to refs. [30–34], $ECOP$ of the cycle is defined as follows:

$$ECOP = \frac{P_2}{T_0 \sigma_{un2}} \tag{48}$$

The E_{un} is defined as follows:

$$E_{un2} = P_2 - T_0 \sigma_{un2} \tag{49}$$

3. Optimization Development: Evolutionary algorithm

3.1. Genetic algorithm

Genetic algorithms provide the best suitable answer of the studding system employing a repetitious and random exploration approach and duplicate it by simple basics of biological evolution [72]. The individual that is a possible solution to the optimization case [73] presents the values of the decision elements. More explanations about Genetic algorithms and its function is available in References [72, 73].

Results and Discussions

4.1 Performance analyses for the condition *n* less than *k*

Fig.2 depicts the impact of n on the performance relations among power, efficiency and compression ratio. It is evident that as ε increases, P1 and η1 initially increase and finally decrease. It should be noted that that P1,max and η1,max do not take place at the same time. On the other hand, P1,max and η1,max increase by the enhancement of n. Furthermore, the efficiency at maximum power rises by the enhancement of n.

Preprints (www.preprints.org) | NOT PEER-REVIEWED | Posted: 9 May 2019 doi:10.20944/preprints201905.0100.v1

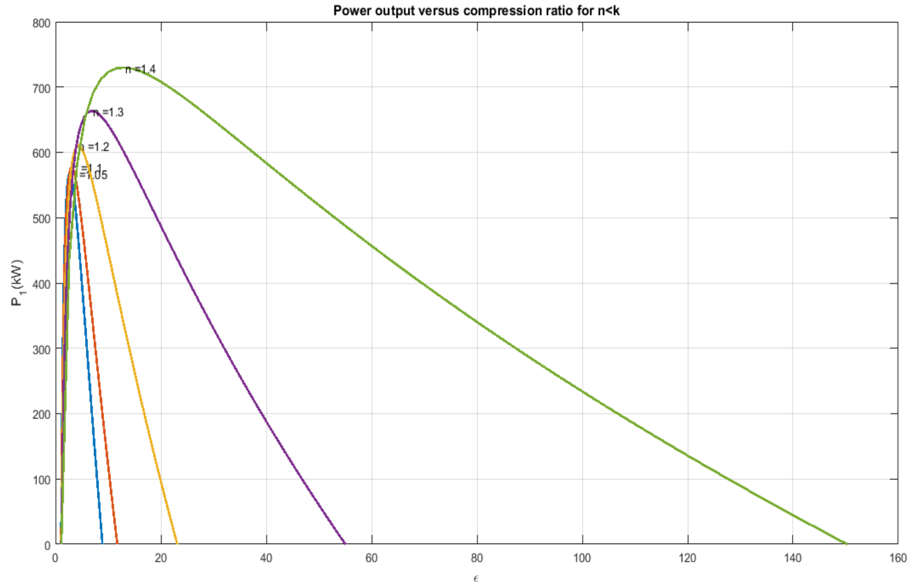

(a)

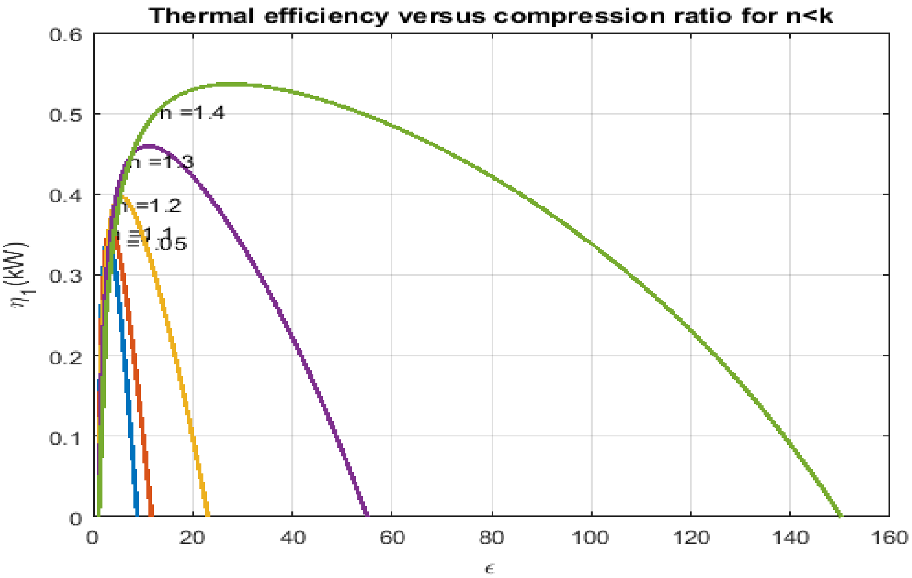

(b)

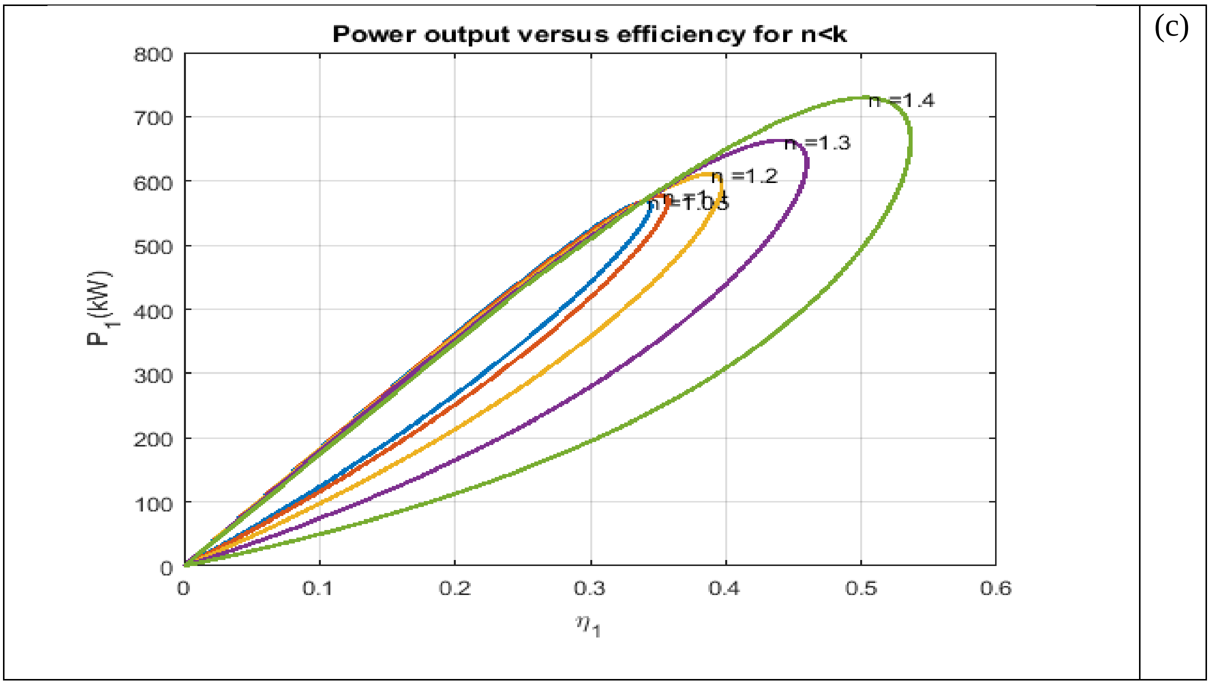

Fig.2 Impact of n ($n<k$) on P_1 - ε (a), η_1 - ε (b) and P_1- η_1 (c) relations.

Fig.3 illustrates the impact of ρ on the relationship between P1 and ε at n = 1.2.

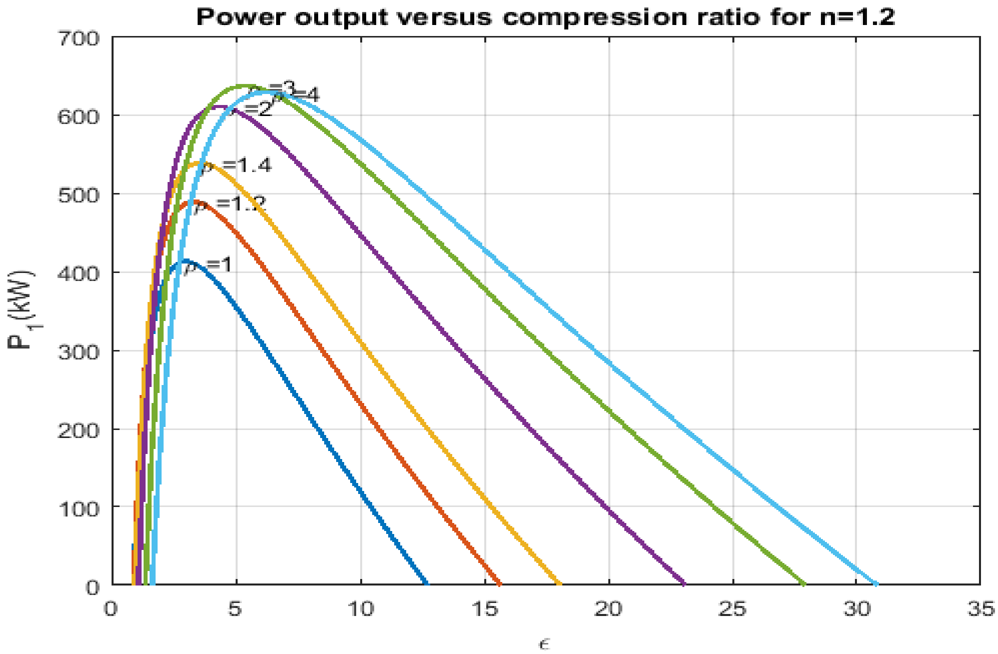

Fig.3 Effect of ρ on P_1 versus ε (n=1.2).

Fig.4 depicts the E_{un} changes against P1 and $\eta 1$ relations at various n. It is obvious that n has a direct relationship with P1 and $\eta 1$. The maximum E_{un} point is adjacent to P1,max and $\eta 1$, max. In other words, optimum values of P1 and $\eta 1$ could be achieved when E_{un} is optimized.

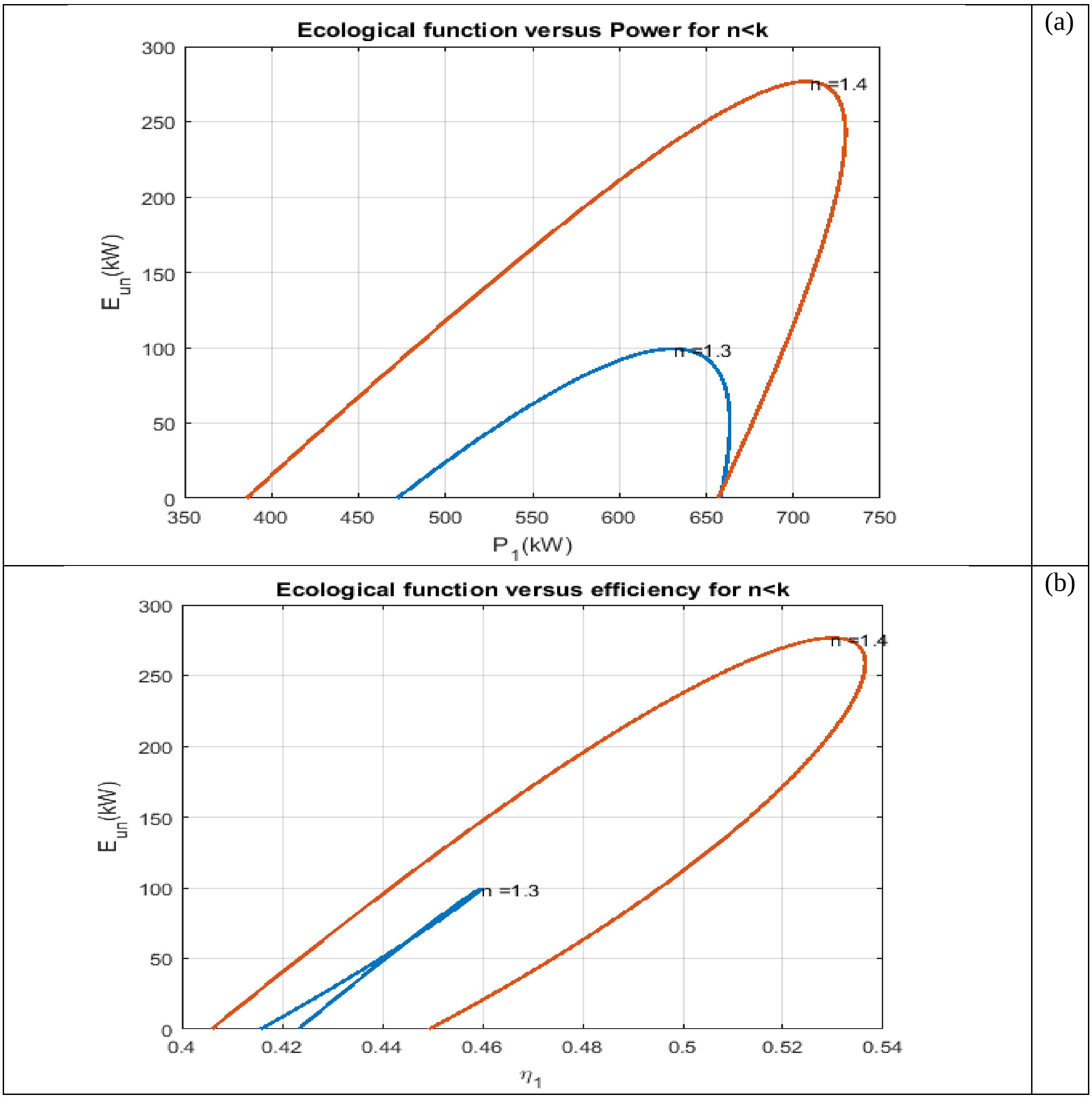

Figure 4 Impact of (n<k) n on E_{un} - P_1 (a) and E_{un} - η_1 (b).

As shown in Fig. 5a. As the compression ratio increases, with a very steep gradient, *ECOP* first increases to its maximum point and then begins to decrease. Also, in a constant compression, the *ECOP* increases with the increase of the n (n<k). Figures 5b and 5c show that the maximum value of the coefficient of performance for various n (n<k) will occur at almost the maximum power and maximum thermal efficiency.

 doi:10.20944/preprints201905.0100.v1

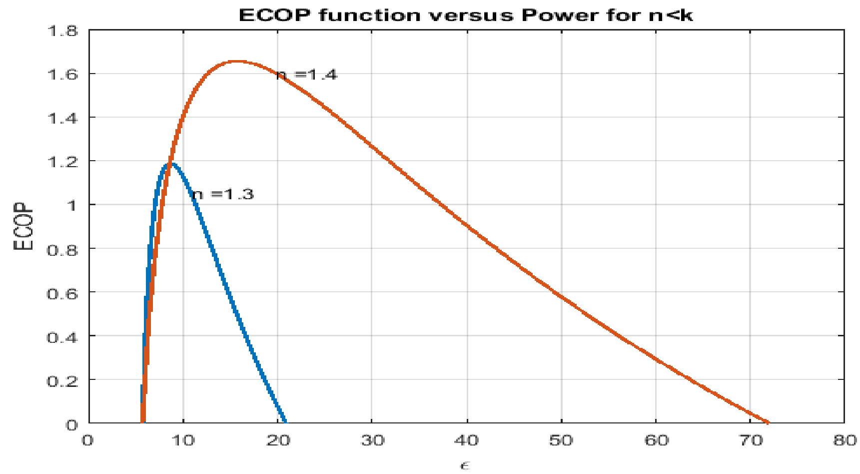

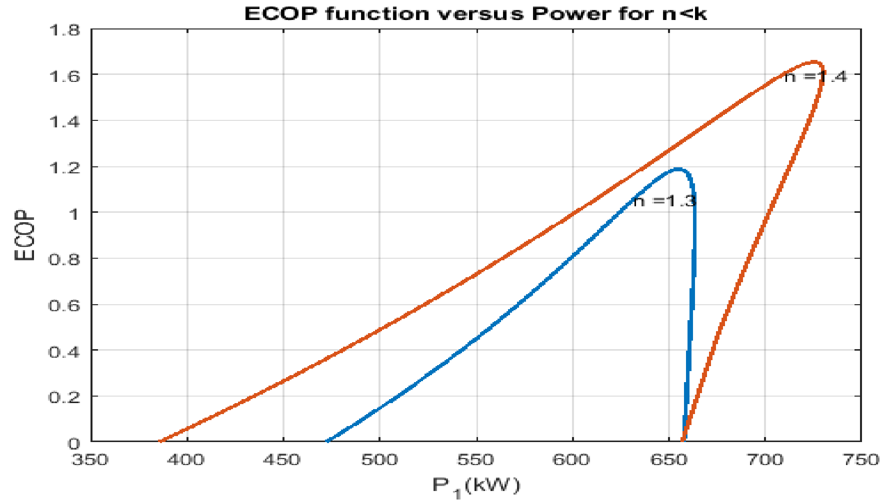

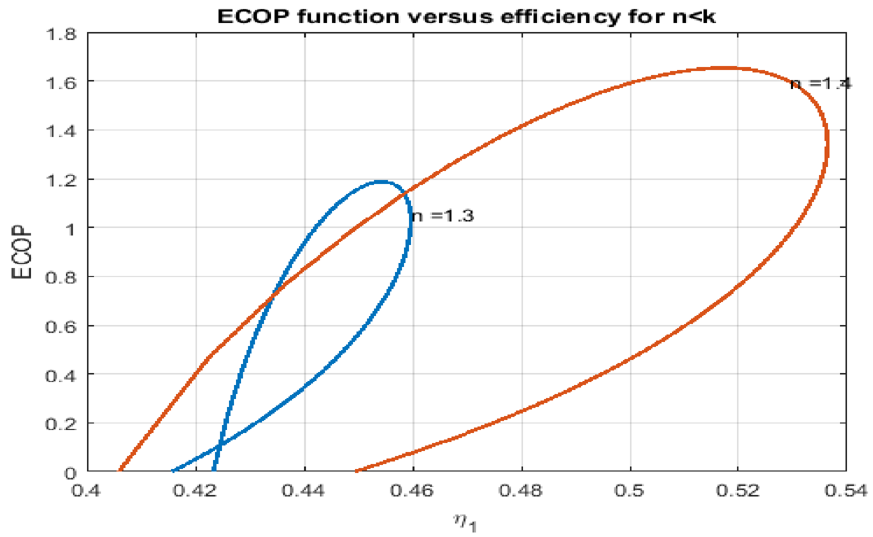

Fig.5 Impact of *n* (*n*<*k*) on *ECOP* - ε (a), *ECOP* - P_1 (b) and *ECOP* - η_1 (c).

4.2 Performance evaluation at the condition of *n* higher than *k*

Fig.6 depicts the impact of n on the performance relations among power, efficiency and compression ratio. It is obvious that when ε increases, P1 and η1 initially increase and finally

Preprints (www.preprints.org) | NOT PEER-REVIEWED | Posted: 9 May 2019 doi:10.20944/preprints201905.0100.v1

decrease. Enhancing n leads to slowly reduction of P2 and $\eta 2$. It should be noted that P2, max and $\eta 2$,max, do not take place at the same value of epsilon . Hence, the $\eta 2$ at P2, max reduces by enhancement of n.

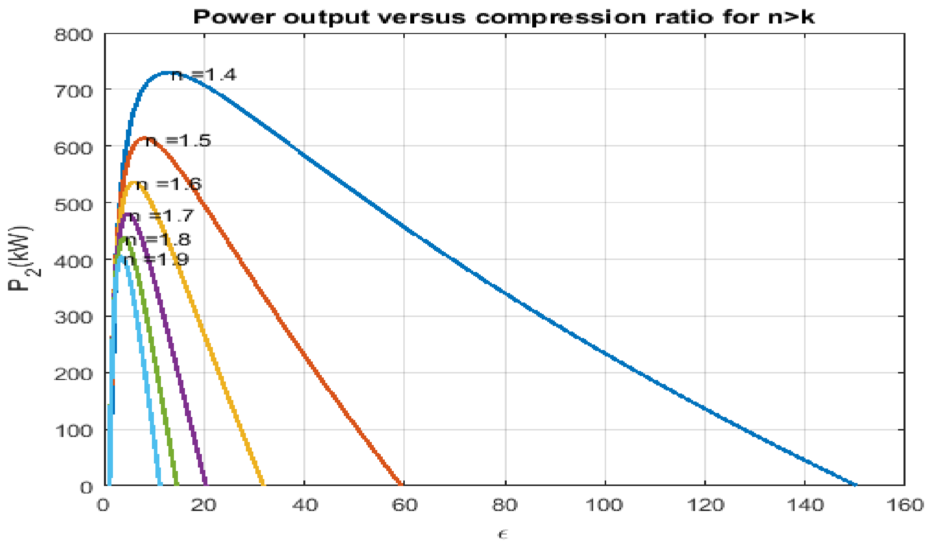

(a)

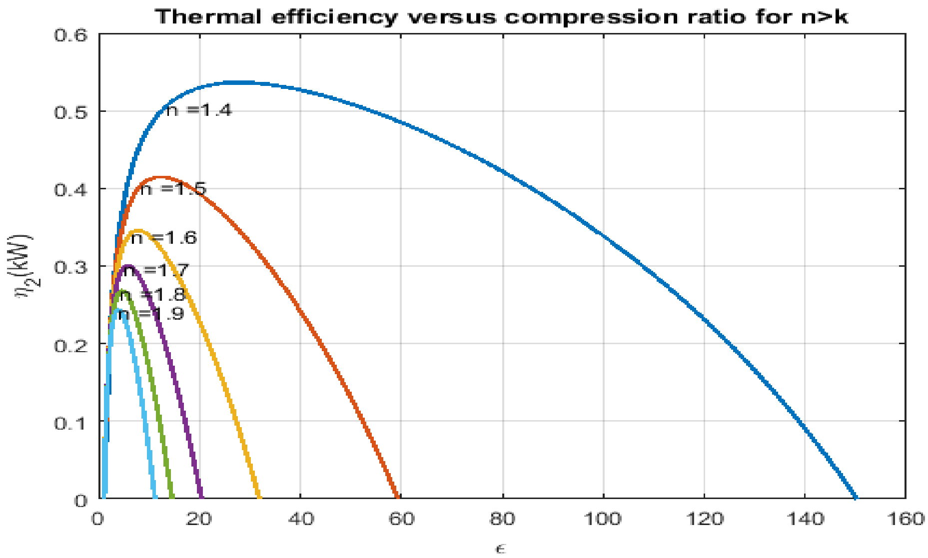

(b)

Preprints (www.preprints.org) | NOT PEER-REVIEWED | Posted: 9 May 2019 doi:10.20944/preprints201905.0100.v1

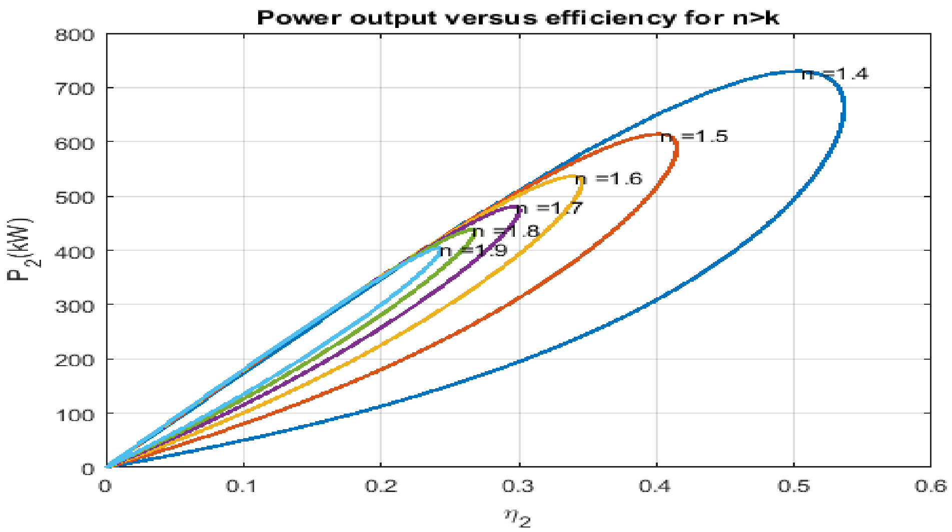

(c)

Fig.6 Impact of *n* (*n*>*k*) on P_2 - ε (a), η_2 - ε (b) and P_2 - η_2 (c).

Fig.7 illustrates the impact of ρ on the relationship between P2 and ε at n = 1.6.

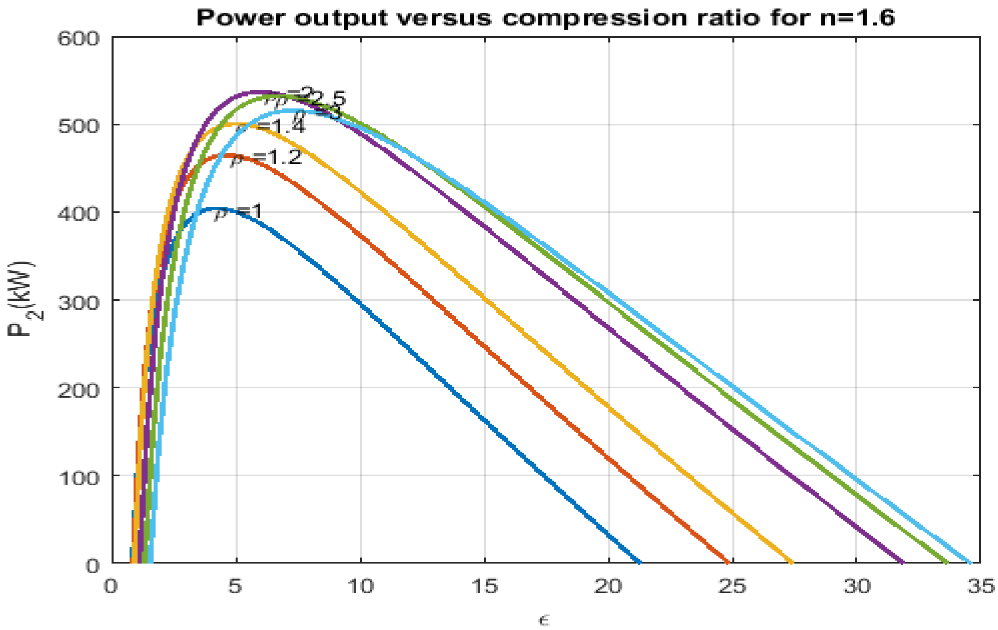

Fig.7 Effect of ρ on P_2 against ε (*n*=1.6).

Figure 8 presents the E_{un} impact on P2 and η2 at various n. It is obvious that increasing n leads to E_{un} , and E_{un} reduction. The E_{un} ,max is adjacent to P2,max and η2,max. In other words, optimum values of P2 and η2 could be achieved when E_{un} is optimized.

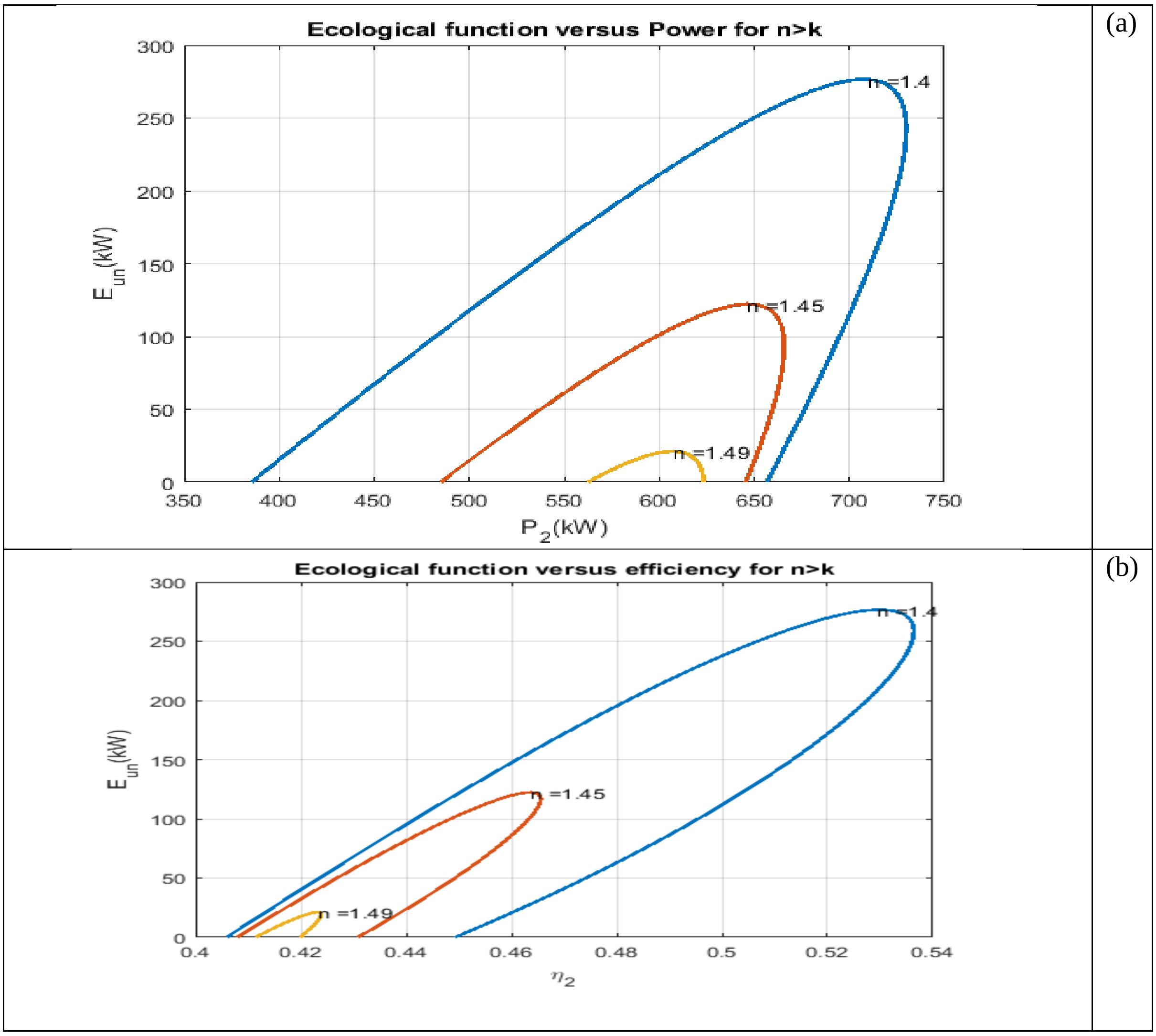

Fig.8 Impact of n ($n>k$) on $ECOP - P_2$ (a) and on $ECOP - \eta_2$ (b).

As shown in Fig. 9a. As the compression ratio increases, with a very steep gradient, the $ECOP$ first increases to its maximum point and then begins to decrease. In addition, in a constant compression, the $ECOP$ decreases with the increase of the n ($n>k$). Figures 9b and 9c show that the maximum value of the coefficient of performance for various n ($n>k$) will occur at almost the maximum power and maximum thermal efficiency.

(a)

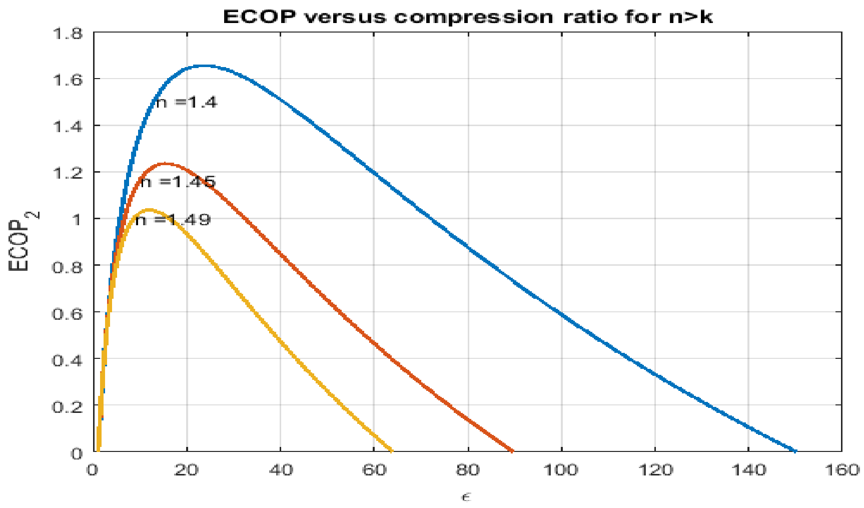

(b)

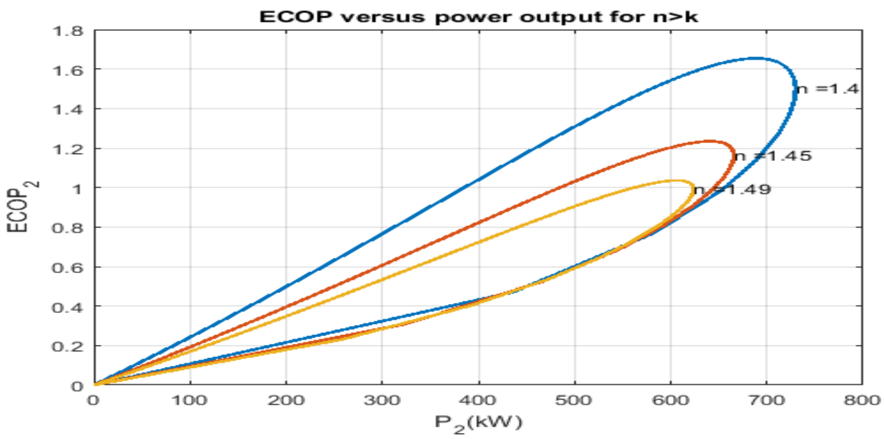

(c)

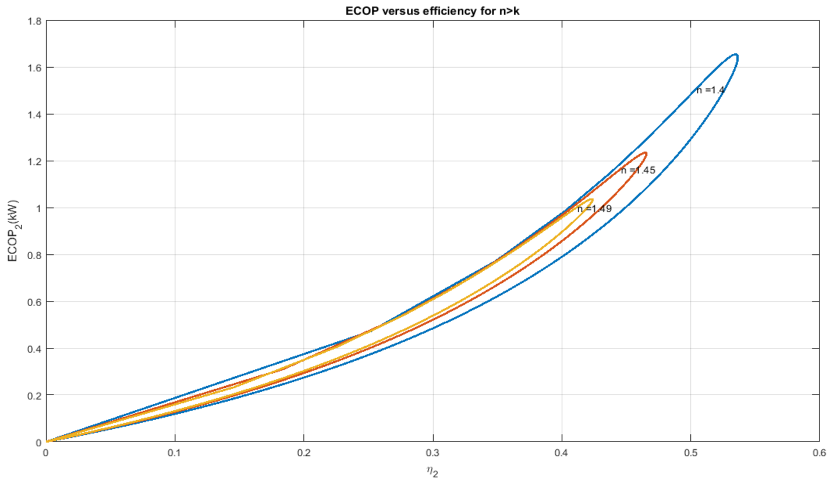

Fig.9 Affect of n ($n>k$) on $ECOP$ - ε (a), $ECOP - P_2$ (b) and $ECOP - \eta_2$ (c).

4.3. Optimization results for *n* less than *k*

Preprints (www.preprints.org) | NOT PEER-REVIEWED | Posted: 9 May 2019 doi:10.20944/preprints201905.0100.v1

Three objective functions are utilized in this optimization: η_1, *ECOP* and E_{un1}, described by Eqs. (26), (30) and (31), respectively. Also, tree decision variables are considered: ε, ρ and n.

Although the decision variables might be various in the optimizing plan, but they typically need to be fitted in a sensible range. Thus, the objective functions are determined by relative limits:

$$18 \le \varepsilon \le 25 \tag{50}$$

$$1.5 \le \rho \le 1.8 \tag{51}$$

$$1.2 \le n \le 1.4 \tag{52}$$

In this study η_1, *ECOP* and E_{un1} of the dual Miller cycle are maximized concurrently employing multi-objective optimization by the mean of the NSGA-II approach. The objective functions are illustrated by Eqs. (26), (30) and (31) and the limitations by Eqs. (50) -(52).

The decision parameters of optimization are as follow: ε, ρ and n. The Pareto optimal frontier of objective functions (the thermal efficiency, *ECOP* and E_{un1}) is depicted in Fig. 10. Selected points with different decision-making methods are presented, as well.

Preprints (www.preprints.org) | NOT PEER-REVIEWED | Posted: 9 May 2019 doi:10.20944/preprints201905.0100.v1

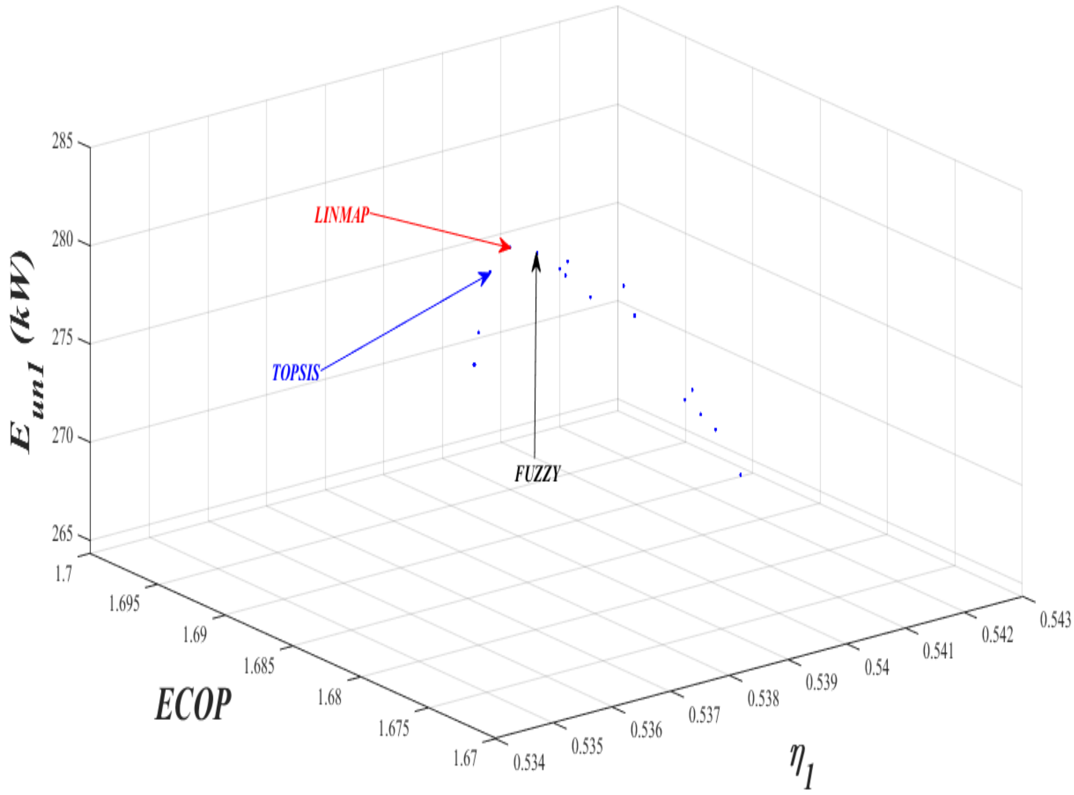

Fig.10.The distribution of the Pareto optimal frontier

Table 1 outlines and compares the optimal results associated with decision elements and objective functions utilizing LINMAP, TOPSIS, and Bellman-Zadeh decision-making methods.

Table.1. Decision making results of this study ($n<k$).

Decision Making Method	**Decision variables**			**Objectives**		
	ε	ρ	n	η_{th}	$ECOP$	$E_{un}\,(kW)$
TOPSIS	19.45280631	1.685157	1.399998	0.537317	1.684802	280.799447
LINMAP	19.865730	1.640773	1.399866	0.538826	1.689876	279.221015
Fuzzy	20.070760	1.542415	1.399997	0.540668	1.695860	275.572407

Preprints (www.preprints.org) | NOT PEER-REVIEWED | Posted: 9 May 2019 doi:10.20944/preprints201905.0100.v1

4.4. Optimization results for *n* higher than *k*

Three objective functions are utilized in this optimization: η_2, *ECOP* and E_{un2}, described by Eqs. (44), (48) and (49), respectively. Also, tree decision variables are considered: ε, ρ and n.

Although the decision variables might be different in the optimizing plan, but they typically need to be fitted in a sensible range. Thus, the objective functions are determined by relative limits:

$$18 \le \varepsilon \le 25 \tag{53}$$

$$1.5 \le \rho \le 1.8 \tag{54}$$

$$1.4 < n \le 1.6 \tag{55}$$

In this study, η_2, *ECOP* and E_{un2} of the dual Miller cycle are maximized concurrently utilizing multi-objective optimization based on the NSGA-II approach. The objective functions are illustrated by Eqs. (48), (49) and (50) and limitations by Eqs. (53) -(55).

The decision parameters of optimization are as follow: ε, ρ and n. The Pareto optimal frontier of objective functions (the thermal efficiency, *ECOP* and E_{un2}) is depicted in Fig. 11. Selected points with different decision-making methods are presented, as well.

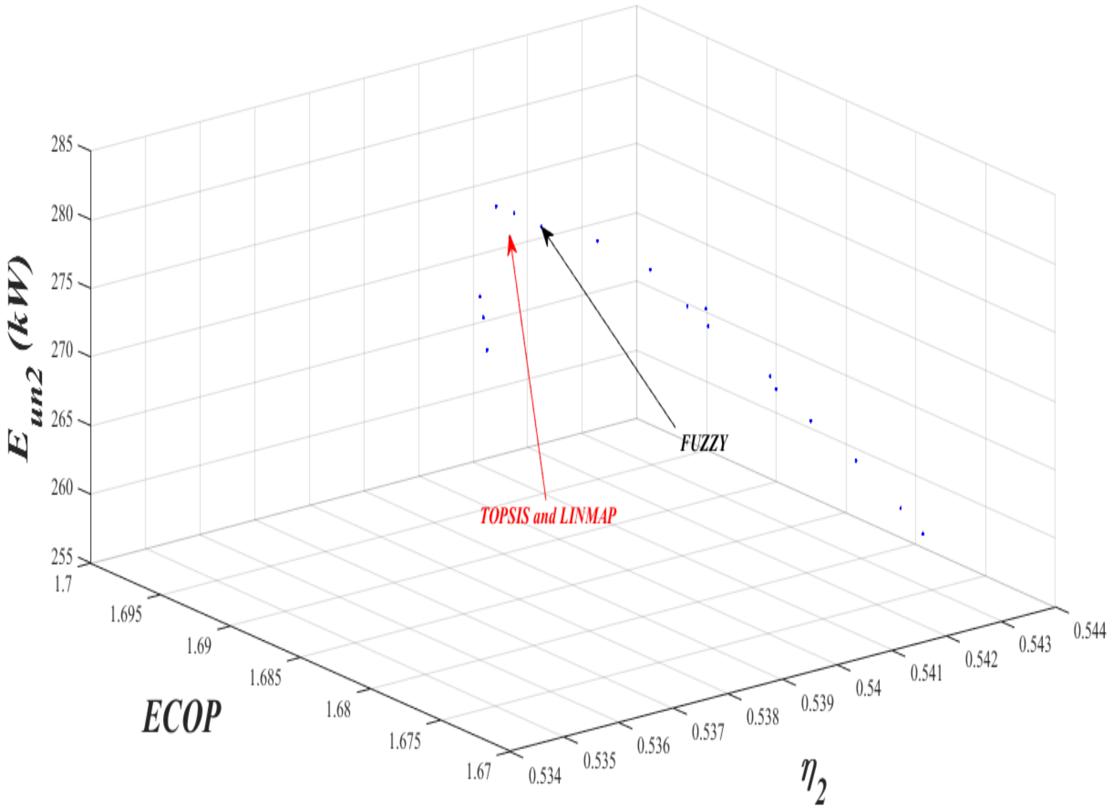

Fig.11.The distribution of the Pareto optimal frontier

Table 2 outlines and compares the optimal results associated with decision elements and objective functions utilizing LINMAP, TOPSIS, and Bellman-Zadeh decision-making methods.

Table.2. Decision making results of this study ($n>k$).

Decision Making Method	**Decision variables**			**Objectives**		
	ε	ρ	n	η_{th}	$ECOP$	$E_{un}\,(kW)$
TOPSIS	20.218658	1.687013	1.400023	0.538473	1.687494	279.731477
LINMAP	20.218658	1.687013	1.400023	0.538473	1.687494	279.731477
Fuzzy	20.382900	1.524323	1.400026	0.541197	1.695881	273.780793

5. Conclusions

A thermodynamic optimization has been carried to obtain the thermal efficiency, *ECOP* and E_{un} of the Dual-Miller Cycle. The compression ratio, the cut-off ratio, and the polytropic index are examined by the NSGA-II approach. Employing various decision-making methods (LINMAP, TOPSIS and fuzzy), the best optimum answer selected from the Pareto frontier. The study achieved a promising and satisfactory state of operation for Dual-Miller systems. The three methods give closed results (with a relative difference less than 3% on compression ratio, 5% on cut-off ratio, 2% on the objective function.

References

[1] Andresen B. Finite-Time Thermodynamics. Physics Laboratory II. University of Copenhagen, 1983

[2] Andresen B, Berry R S, Ondrechen M J, et al. Thermodynamics for processes in finite time. Acc Chem Res, 1984, 17: 266–271

[3] Bejan A. Entropy generation minimization: The new thermodynamics of finite-size devices and finite-time processes. J Appl Phys, 1996, 79: 1191–1218

[4] Berry R S, Kazakov V A, Sieniutycz S, et al. Thermodynamic Optimization of Finite Time Processes. Chichester: Wiley, 1999

[5] Chen L G, Wu C, Sun F R. Finite time thermodynamic optimization or entropy generation minimization of energy systems. J Non-Equilib Thermodyn, 1999, 24: 327–359

[6] Salamon P, Nulton J D, Siragusa G, et al. Principles of control thermodynamics. Energy, 2001, 26: 307–319

[7] Chen L G, Sun F R. Advances in Finite Time Thermodynamics: Analysis and optimization. New York: Nova Science Publishers, 2004

[8] Chen L G. Finite Time Thermodynamic Analysis of Irreversible Process and Cycles (in Chinese). Beijing: Higher Education Press, 2005

[9] Sieniutycz S, Jezowski J. Energy Optimization in Process Systems. Oxford, UK: Elsevier, 2009

[10] Andresen B. Current trends in finite-time thermodynamics. Angew Chem Int Ed, 2011, 50: 2690–2704

[11] Wu F, Chen L G, Sun F R, et al. Finite Time Thermodynamic Optimization of Stirling Machine (in Chinese). Beijing: Chemical Industry Press, 2008

[12] Sieniutycz S, Jezowski J. Energy Optimization in Process Systems and Fuel Cells. Oxford, UK: Elsevier, 2013

[13] Medina A, Curto-Risso P L, Calvo-Hernández A, et al. Quasi-Dimensional Simulation of Spark Ignition Engines. From Thermodynamic Optimization to Cyclic Variability. London: Springer, 2014

[14] Ding Z M, Chen L G, Wang W H, et al. Advances in finite time thermodynamic performance optimization of three kinds of micro energy conversion systems (in Chinese). Sci Sin Tech, 2015, 45: 889–918

[15] Hoffmann K H, Andresen B, Salamon P. Finite-time thermodynamics tools to analyze dissipative processes. In: Dinner A R, Eds. Proceedings of the 240 Conference: Science's Great Challences, Advances in Chemical Physics. Volume 157. New Jersey: Wiley, 2015. 57–67

[16] Ahmadi M H, Ahmadi M A, Sadatsakkak S A. Thermodynamic analysis and performance optimization of irreversible Carnot refrigerator by using multi-objective evolutionary algorithms (MOEAs). Renew Sust Energ Rev, 2015, 51: 1055–1070

[17] Chen L G, Meng F K, Sun F R. Thermodynamic analyses and optimization for thermoelectric devices: The state of the arts. Sci China Tech Sci, 2016, 59: 442–455

[18] Chen L, Feng H, Xie Z. Generalized thermodynamic optimization for iron and steel production processes: Theoretical exploration and application cases. Entropy, 2016, 18: 353

[19] Sieniutycz S. Thermodynamic Approaches in Engineering Systems. Oxford: Elsevier, 2016

[20] Chen L G, Xia S J. Generalized Thermodynamics Dynamic Optimization of Irreversible Processes (in Chinese). Beijing: Science Press, 2016

[21] Chen L G, Xia S J. Generalized Thermodynamics Dynamic Optimization of Irreversible Cycles (in Chinese). Beijing: Science Press, 2016

[22] Bi Y H, Chen L G. Finite time thermodynamic optimization of air heat pump performance (in Chinese). Beijing: Science Press, 2017

[23] Ahmadi M H, Ahmadi M A, Pourfayaz F. Thermal models for analysis of performance of Stirling engine: A review. Renew Sust Energ Rev, 2017, 68: 168–184

[24] Ge Y, Chen L, Sun F. Progress in finite time thermodynamic studies for internal combustion engine cycles. Entropy, 2016, 18: 139

[25] Chen L, Zhang W, Sun F. Power, efficiency, entropy-generation rate and ecological optimization for a class of generalized irreversible universal heat-engine cycles. Appl Energy, 2007, 84: 512–525

[26] Zhou B, Cheng X T, Liang X G. Power output analyses and optimizations of the Stirling cycle. Sci China Tech Sci, 2013, 56: 228–236

[27] Ge Y, Chen L, Sun F. Optimal path of piston motion of irreversible Otto cycle for minimum entropy generation with radiative heat transfer law. J Energy Inst, 2012, 85: 140–149

 doi:10.20944/preprints201905.0100.v1

[28] Wang C, Chen L, Xia S, et al. Optimal concentration configuration of consecutive chemical reaction A ⇔ B ⇔ C for minimum entropy generation. J Non-Equilib ThermoDyn, 2016, 41: 313–326

[29] Wu Y Q. Analyses of thermodynamic performance for the endoreversible Otto cycle with the concepts of entropy generation and entransy. Sci China Tech Sci, 2017, 60: 692–700

[30] Angulo-Brown F. An ecological optimization criterion for finite-time heat engines. J Appl Phys, 1991, 69: 7465–7469

[31] Yan Z J. Comment on "ecological optimization criterion for finite time heat engines". *J Appl Phys*, 1993, 73: 3583

[32] Angulo-Brown F, Fernández-Betanzos J, Diaz-Pico C A. Compression ratio of an optimized air standard Otto-cycle model. Eur J Phys, 1994, 15: 38–42

[33] Chen L G, Sun F R, Chen W Z. The ecological quality factor for thermodynamic cycles (in Chinese). J Eng Therm Energy Power, 1994, 9: 374–376

[34] Long R, Li B, Liu Z, et al. Ecological analysis of a thermally regenerative electrochemical cycle. Energy, 2016, 107: 95–102

[35] Üst Y, Sahin B, Kodal A. Ecological coefficient of performance (ECOP) optimization for generalized irreversible Carnot heat engines. J Energy Inst, 2005, 78: 145–151

[36] Ust Y, Sahin B, Sogut O S. Performance analysis and optimization of an irreversible dual-cycle based on an ecological coefficient of performance criterion. Appl Energy, 2005, 82: 23–39

[37] Ust Y, Sahin B, Kodal A. Performance analysis of an irreversible Brayton heat engine based on ecological coefficient of performance criterion. Int J Thermal Sci, 2006, 45: 94–101

[38] Ust Y. Performance analysis and optimization of irreversible air refrigeration cycles based on ecological coefficient of performance criterion. Appl Thermal Eng, 2009, 29: 47–55

[39] Gonca G, Sahin B. Performance optimization of an air-standard irreversible dual-Atkinson cycle engine based on the ecological coefficient of performance criterion. Sci World J, 2014, 2014: 1–10

[40] Ust Y, Sahin B, Cakir M. Ecological coefficient of performance analysis and optimisation of gas turbines by using exergy analysis approach. Int J Exergy, 2016, 21: 39–69

[41] Salamon P, Hoffmann K H, Schubert S, et al. What conditions make minimum entropy production equivalent to maximum power production? J Non-Equilib Thermodyn, 2001, 26: 73–83

[42] Blank D A, Wu C. The effects of combustion on a power-optimized endoreversible Dual cycle. Energy Conv Manag, 1994, 14: 98–103

[43] Chen L, Sun F, Wu C. Optimal performance of an irreversible dual cycle. Appl Energy, 2004, 79: 3–14

[44] Ust Y, Sahin B, Kayadelen H K, et al. Heat transfer effects on the performance of an air-standard irreversible dual cycle. Int J Vehicle Des, 2013, 63: 102

[45] Ghatak A, Chakraborty S. Effect of external irreversibilities and variable thermal properties of working fluid on thermal performance of a Dual internal combustion engine cycle. Strojnicky Casopsis (J Mech Energy), 2007, 58: 1–12

[46] Wang W, Chen L, Sun F, et al. The effect of friction on the performance of an air standard dual cycle. Exergy An Int J, 2002, 2: 340–344

[47] Ge Y, Chen L, Sun F. Finite-time thermodynamic modeling and analysis for an irreversible Dual cycle. Math Comp Model, 2009, 50: 101–108

[48] Al-Sarkhi A, Akash B A, Jaber J O, et al. Efficiency of Miller engine at maximum power density. Int Commun Heat Mass Transfer, 2002, 29: 1159–1167

[49] Chen L G, Ge Y L, Sun F R, et al. The performance of a Miller cycle with heat transfer, friction and variable specific heats of working fluid. Termotehnica, 2010, 14: 24–32

[50] Chen L, Ge Y, Sun F, et al. Finite-time thermodynamic modelling and analysis for an irreversible Miller cycle. Int J Ambient Energy, 2011, 32: 87–94

[51] Lin J, Xu Z, Chang S, et al. Finite-time thermodynamic modeling and analysis of an irreversible Miller cycle working on a four-stroke engine. Int Commun Heat Mass Transfer, 2014, 54: 54–59

[52] Gonca G, Sahin B, Ust Y, et al. Comparison of steam injected diesel engine and Miller cycled diesel engine by using two zone combustion model. J Energy Inst, 2015, 88: 43–52

[53] Gonca G, Sahin B, Parlak A, et al. Theoretical and experimental investigation of the Miller cycle diesel engine in terms of performance and emission parameters. Appl Energy, 2015, 138: 11–20

[54] Ebrahimi R. Second law analysis on an air-standard miller engine. Acta Phys Pol A, 2016, 129: 1079–1082

[55] Mousapour A, Hajipour A, Rashidi M M, et al. Performance evaluation of an irreversible Miller cycle comparing FTT (finite-time thermodynamics) analysis and ANN (artificial neural network) prediction. Energy, 2016, 94: 100–109

[56] Zhao J. Research and application of over-expansion cycle (Atkinson and Miller) engines—A review. Appl Energ, 2017, 185: 300–319

[57] Gonca G, Sahin B, Ust Y. Performance maps for an air-standard irreversible Dual-Miller cycle (DMC) with late inlet valve closing (LIVC) version. Energy, 2013, 54: 285–290

[58] Gonca G, Sahin B, Ust Y. Investigation of heat transfer influences on performance of air-standard irreversible Dual-Miller cycle. J Thermophys Heat Transfer, 2015, 29: 678–683

[59] Gonca G. Comparative performance analyses of irreversible OMCE (Otto Miller cycle engine)-DiMCE (Diesel miller cycle engine)-DMCE (Dual Miller cycle engine). Energy, 2016, 109: 152–159

[60] Ust Y, Arslan F, Ozsari I, et al. Thermodynamic performance analysis and optimization of DMC (Dual Miller Cycle) cogeneration system by considering exergetic performance coefficient and total exergy output criteria. Energy, 2015, 90: 552–559

Preprints (www.preprints.org) | NOT PEER-REVIEWED | Posted: 9 May 2019 doi:10.20944/preprints201905.0100.v1

[61] Gonca G. Thermo-ecological analysis of irreversible Dual-Miller Cycle (DMC) engine based on the ecological coefficient of performance (ECOP) criterion. Iran J Sci Tech Trans Mech Eng, 2016: 1–12

[62] Gonca G, Sahin B. Thermo-ecological performance analyses and optimizations of irreversible gas cycle engines. Appl Thermal Eng, 2016, 105: 566–576

[63] Wu Z X, Chen L G, Ge Y L, et al. Ecological objective function optimization of an irreversible Dual-Miller cycle with linear variable specific heat ratio of the working fluid (in Chinese). Energy Conser, 2016, 6: 20–27

[64] Wu Z X, Chen L G, Ge Y L, et al. Power, efficiency, ecological function and ecological coefficient of performance of an irreversible Dual-Miller cycle (DMC) with nonlinear variable specific heat ratio of working fluid. Euro Phys J Plus, 2017, 132: 209

[65] Huleihil M, Mazor G. Irreversible performance characteristics of air standard Otto cycles with polytropic processes. Appl Mech Eng, 2012, 1: 1000111

[66] Gong S W, Chen L G, Sun F R. Performance analysis and optimization of endoreversible Lenoir cycle with polytropic process (in Chinese). Energy Conser, 2013, 32: 22–26

[67] Xiong B, Chen L G, Ge Y L, et al. Finite-time thermodynamic analysis of an endoreversible Otto cycle with polytropic process (in Chinese). Power Energy, 2014, 35: 166–171

[68] Zhang K, Chen L G, Qin X Y, et al. Finite time thermodynamic analysis of irreversible universal reciprocating cycle with polytropic process (in Chinese). Energy Conser, 2015, 34: 15–21

[69] T. Özyer, M. Zhang, R. Alhajj, Integrating multi-objective genetic algorithm based clustering and data partitioning for skyline computation, Appl Intell, 35 (2011),pp.110-122.

[70] O. Beatrice, J.R. Brian, H. Franklin, Multi-Objective Genetic Algorithms for Vehicle Routing Problem with Time Windows, Applied Intelligence, 24 (2006),pp.17-30.

[71] I. Blecic, A. Cecchini, G. Trunfio, A decision support tool coupling a causal model and a multi-objective genetic algorithm, Appl Intell, 26 (2007) , pp.125-137.

[72] D.A.V. Veldhuizen, G.B. Lamont, Multi objective Evolutionary Algorithms Analyzing the State-of-the-Art, (2000).

[73] A. Konak, D.W. Coit, A.E. Smith, Multi-objective optimization using genetic algorithms: A tutorial, Reliability Engineering & System Safety, 91 (2006),pp. 992-1007.

[74] Ahmadi MH, Hosseinzade H, Sayyaadi H, Mohammadi AH, Kimiaghalam F. Application of the multi-objective optimization method for designing a powered Stirling heat engine: design with maximized power, thermal efficiency and minimized pressure loss. Renew Energy 2013(60), pp. 313–22.

[75] Ahmadi MH, Sayyaadi H, Mohammadi AH, Marco A. Barranco-Jimenez. Thermo-economic multi-objective optimization of solar dish-Stirling engine by implementing evolutionary algorithm, Energy Conversion and Management,73(2013), pp. 370–380

[76] Ahmadi MH, Sayyaadi H, Dehghani S, Hosseinzade H. Designing a solar powered Stirling heat engine based on multiple criteria: Maximized thermal efficiency and power., Energy Conversion and Management,75(2013), pp. 282–291

[77] Ahmadi MH, Dehghani S, Mohammadi AH, Feidt M, Marco A. Barranco-Jimenez. Optimal design of a solar driven heat engine based on thermal and thermo-economic criteria, Energy Conversion and Management (2013); 75,635–642.

[78] Sayyaadi H., Ahmadi M.H., Dehghani S. (2014). "Optimal Design of a Solar-Driven Heat Engine Based on Thermal and Ecological Criteria." J. Energy Eng. , 10.1061/(ASCE)EY.1943-7897.0000191 , 04014012.

[79] A. Lazzaretto, A. Toffolo, Energy, economy and environment as objectives in multi-criterion optimization of thermal systems design, Energy, 29 (2004),pp. 1139-1157.

[80] Ahmadi, M. H., Mohammadi A. H., Pourkiaei S. M., (2014). “Optimisation of the thermodynamic performance of the Stirling engine.” International Journal of Ambient Energy, DOI: 10.1080/01430750.2014.907211

[81] A. Toffolo, A. Lazzaretto, Evolutionary algorithms for multi-objective energetic and economic optimization in thermal system design, Energy, 27 (2002), pp.549-567.

[82] Ahmadi MH., Mohammadi AH., Dehghani S. (2013) Evaluation of the maximized power of a regenerative endoreversible Stirling cycle using the thermodynamic analysis, Energy Conversion and Management.76, 561–570.

[83] Ahmadi, M.H.,Ahmadi, M.A., Feidt, M.‘‘Performance Optimization of a Solar-Driven Multi-Step Irreversible Brayton Cycle Based on a Multi-Objective Genetic Algorithm’’, Oil Gas Sci. Technol.—Rev. IFP., DOI: 10.2516/ogst/2014028 (2014).

[84] Ahmadi M.H., Ahmadi M.A, Mehrpooya M.,Hosseinzade H. , Feidt M., Thermodynamic and thermoeconomic analysis and optimization of performance of irreversible four-temperature-level absorption refrigeration, Energy Conversion and Management 88 (2014) 1051–1059.

[85] Ahmadi M.H., Ahmadi M.A, Thermodynamic analysis and optimization of an irreversible Ericsson cryogenic refrigerator cycle, Energy Conversion and Management 89 (2015) 147–155.

[86] Mohammad H. Ahmadi , Mohammad Ali Ahmadi (2014), Thermodynamic analysis and optimisation of an irreversible radiative-type heat engine by using non-dominated sorting genetic algorithm, International Journal of Ambient Energy, DOI: 10.1080/01430750.2014.977498.

[87] MH Ahmadi , MA Ahmadi, M Mehrpooya, M. Sameti, Thermo-ecological analysis and optimization performance of an irreversible three-heat-source absorption heat pump, Energy Conversion and Management 90 (2015) 175–183.

[88] Hooshang, Mazdak, Somayeh Toghyani, Alibakhsh Kasaeian, Reza Askari Moghadam, and Mohammad Hossein Ahmadi. "Enhancing and multi-objective optimising of the performance of Stirling engine using third-order thermodynamic analysis." *International Journal of Ambient Energy* 39, no. 4 (2018): 382-391.

[89] Ahmadi, Mohammad H., Mohammad Ali Jokar, Tingzhen Ming, Michel Feidt, Fathollah Pourfayaz, and Fatemeh Razi Astaraei. "Multi-objective performance optimization of irreversible molten carbonate fuel cell–Braysson heat engine and thermodynamic analysis with ecological objective approach." *Energy* 144 (2018): 707-722.

[90] Jokar, Mohammad Ali, Mohammad H. Ahmadi, Mohsen Sharifpur, Josua P. Meyer, Fathollah Pourfayaz, and Tingzhen Ming. "Thermodynamic evaluation and multi-objective optimization of molten carbonate fuel cell-supercritical CO2 Brayton cycle hybrid system." *Energy Conversion and Management* 153 (2017): 538-556.

[91] Ahmadi, Mohammad H., Mehdi Mehrpooya, Sara Abbasi, Fathollah Pourfayaz, and Joan Carles Bruno. "Thermo-economic analysis and multi-objective optimization of a transcritical CO2 power cycle driven by solar energy and LNG cold recovery." *Thermal Science and Engineering Progress* 4 (2017): 185-196.

[92] Ahmadi, Mohammad H., Mohammad-Ali Ahmadi, Akbar Maleki, Fathollah Pourfayaz, Mokhtar Bidi, and Emin Açıkkalp. "Exergetic sustainability evaluation and multi-objective optimization of performance of an irreversible nanoscale Stirling refrigeration cycle operating with Maxwell–Boltzmann gas." *Renewable and Sustainable Energy Reviews* 78 (2017): 80-92.

[93] Ahmadi, Mohammad H., Mehdi Mehrpooya, and Fathollah Pourfayaz. "Thermodynamic and exergy analysis and optimization of a transcritical CO2 power cycle driven by geothermal energy with liquefied natural gas as its heat sink." *Applied Thermal Engineering* 109 (2016): 640-652.

[94] Ahmadi, Mohammad Hossein, and Mohammad Ali Ahmadi. "Multi objective optimization of performance of three-heat-source irreversible refrigerators based algorithm NSGAII." *Renewable and Sustainable Energy Reviews* 60 (2016): 784-794.

[95] Ahmadi, Mohammad H., Mohammad Ali Ahmadi, and Fathollah Pourfayaz. "Thermodynamic analysis and evolutionary algorithm based on multi-objective optimization performance of actual power generating thermal cycles." *Applied Thermal Engineering* 99 (2016): 996-1005.

[96] Ahmadi, Mohammad H., Mohammad-Ali Ahmadi, Fathollah Pourfayaz, and Mokhtar Bidi. "Thermodynamic analysis and optimization for an irreversible heat pump working on reversed Brayton cycle." *Energy conversion and management* 110 (2016): 260-267.

[97] Sadatsakkak, Seyed Abbas, Mohammad H. Ahmadi, and Mohammad Ali Ahmadi. "Optimization performance and thermodynamic analysis of an irreversible nano scale Brayton cycle operating with Maxwell–Boltzmann gas." *Energy Conversion and Management* 101 (2015): 592-605.

[98] Ahmadi, Mohammad Hossein, Mohammad Ali Ahmadi, Adel Mellit, Fathollah Pourfayaz, and Michel Feidt. "Thermodynamic analysis and multi objective optimization of performance of solar dish Stirling engine by the centrality of entransy and entropy generation." *International Journal of Electrical Power & Energy Systems* 78 (2016): 88-95.

[99] Ahmadi, Mohammad H., Mohammad Ali Ahmadi, Roham Bayat, Milad Ashouri, and Michel Feidt. "Thermo-economic optimization of Stirling heat pump by using non-dominated sorting genetic algorithm." *Energy Conversion and Management* 91 (2015): 315-322.

 doi:10.20944/preprints201905.0100.v1

[100] Ahmadi, Mohammad H., Mohammad Ali Ahmadi, Amir H. Mohammadi, Michel Feidt, and Seyed Mohsen Pourkiaei. "Multi-objective optimization of an irreversible Stirling cryogenic refrigerator cycle." *Energy Conversion and Management* 82 (2014): 351-360.

[101] Sadatsakkak, Seyed Abbas, Mohammad H. Ahmadi, Roham Bayat, Seyed Mohsen Pourkiaei, and Michel Feidt. "Optimization density power and thermal efficiency of an endoreversible Braysson cycle by using non-dominated sorting genetic algorithm." *Energy Conversion and Management* 93 (2015): 31-39.

[102] You, Jiang, LinGen Chen, ZhiXiang Wu, and FengRui Sun. "Thermodynamic performance of Dual-Miller cycle (DMC) with polytropic processes based on power output, thermal efficiency and ecological function." *Science China Technological Sciences* 61, no. 3 (2018): 453-463.

[103] Klein S A. An explanation for observed compression ratios in internal combustion engines. J Eng Gas Turbines Power, 1991, 113: 511–513

[104] Ge Y, Chen L, Sun F. Ecological optimization of an irreversible Otto cycle. Arab J Sci Eng, 2013, 38: 373–381

[105] Ge Y, Chen L, Sun F, et al. Effects of heat transfer and variable specific heats of working fluid on performance of a Miller cycle. Int J Ambient Energy, 2005, 26: 203–214